Chapter 4

Effect of Internal and External Concentration Polarizations on the Performance of Forward Osmosis Process

Amrit Bhinder, Simin Shabani and Mohtada Sadrzadeh

Additional information is available at the end of the chapter

http://dx.doi.org/10.5772/intechopen.71343

Abstract

Forward osmosis (FO) as an osmotically driven membrane process is severely affected by the concentration polarization phenomenon on both sides of the membrane as well as inside the support layer. Though the effect of internal concentration polarization (ICP) in the porous support on the draw solution side is far more pronounced than that of the external concentration polarization (ECP), still the importance of ECP cannot be neglected. The ECP becomes particularly important when the feed flow rate is enhanced to increase the permeation flux by increasing the agitation and turbulence on the membrane surface. To capture the effect of ECP a suitable value of mass transfer coefficient must be determined. In this chapter, an FO mass transport model that accounts for the presence of both ICP and ECP phenomena is first presented on the basis of solution-diffusion model coupled with diffusion-convection. Then, three methods for the estimation of mass transfer coefficient based on empirical Sherwood (Sh) number correlations, pressure-driven reverse osmosis (RO), and osmosis-driven pressure retarded osmosis (PRO) are proposed. Finally, a methodology for the prediction of water flux through FO membranes using the theoretical model and calculated/measured parameters (hydraulic permeability, salt resistivity of the support layer, and mass transfer coefficient) is presented.

Keywords: forward osmosis, concentration polarization, mass transfer coefficient, reverse osmosis, pressure retarded osmosis

1. Introduction

With the increasing application of membrane-based separation processes in desalination and wastewater treatment, vast efforts have been devoted to making them more energy efficient.

In the hunt of more economical and efficient method, forward osmosis (FO) has been developed as an alternative to the conventional pressure-driven separation processes like reverse osmosis (RO) and nanofiltration (NF) [1–3]. FO is an osmotically driven membrane separation process, where water molecules are transferred from a dilute feed solution to a more concentrated draw solution through a semi-permeable membrane which selectively rejects a broad range of dissolved contaminants in the wastewater [3]. The driving force for water transport is the chemical potential difference between the draw and feed solutions, thus eliminating the use of hydraulic pressure and consequently enhances energy efficiency [4–6].

Besides being energy efficient, FO process is less prone to fouling as compared to pressure-driven NF and RO processes. However, FO suffers from an enhanced concentration polarization effect inside the support layer known as internal concentration polarization (ICP), where the solvent (commonly water) permeates through the support and dilutes the draw concentration at the inner side of the active layer. The ICP reduces the real driving force for mass transfer, thereby reducing the performance of the FO process, significantly [7, 8]. In addition to ICP, FO suffers from an external concentration polarization (ECP). In fact, in a typical pressure driven process, ECP occurs on one side of the membrane (feed side), whereas in the FO, this phenomenon happens on both sides (feed and draw). The polarization that occurs on the feed side is concentrative and is different in nature from the dilutive polarization on the draw side due to incoming permeate flux. The first polarization is called concentrative ECP and the second one that takes places in the draw side is termed as dilutive ECP. The ICP is not affected by the hydrodynamics of the flow and is more severe than the ECP which makes the theoretical study of transport phenomena in an FO process very challenging.

Early attempts to model the mass transfer through an FO membrane was conducted by Lee et al. [9]. They considered the ICP inside the porous support and developed a model to predict the performance of a pressure retarded osmosis (PRO) process. In the PRO process, which is used for energy generation from an osmotic pressure difference, the membranes are oriented in the exact opposite configuration of FO with the active layer facing the draw solution. Later, Loeb et al. [10] followed the same approach and developed a model for the FO process. McCutcheon et al. [11] coupled the boundary layer film theory to capture the effect of ECP on the active layer as well as the ICP in the porous support for both FO and PRO processes. Suh and Lee [12] fine-tuned this model by considering the dilutive ECP phenomenon on the draw side which was neglected by previous researchers. They suggested that the effect of diluted draw solution on the ECP must be taken into account, particularly for low cross-flow velocities and high water flux. Even though the above models provide a comprehensive framework of relationships for the ICP and ECP on both sides of FO membranes and can predict the flux satisfactorily at a particular flow rate, they are not sufficiently sensitive to a change in the feed flow rate.

The change in water flux with a change in the flow rate is captured by the mass transfer coefficient (k) on either side of the membrane. The mass transfer coefficient is commonly calculated using Sherwood (Sh) number relations which are empirical correlations as a function of Reynolds Schmidt numbers [13]. The Sh number relationships available in the literature were either adapted from the analogy between heat and mass transfer or were derived for flow in

non-porous smooth [13–15]. These relations were later modified for the ultrafiltration (UF) experiments [13, 14]. UF is a pressure-driven process with a different flow hydrodynamics from FO process which is driven by the osmotic pressure gradient. Also, the topology of a typical UF membrane is rougher (on a microscopic scale) and porous than an FO membrane that might affect the Sh number which is a linear function of a frictional factor. Hence, the correlations of Sh number derived from UF experiments may not be valid for the FO process.

Although extensive research has been carried out on the derivation of empirical and semi-empirical Sh number correlations for pressure driven membrane processes (at various operating conditions and spacer geometries) [14, 16, 17], no such efforts have been made to better understand the boundary layer phenomena in an FO process. It is worth mentioning that, based on the film theory the severity of the ECP depends upon the value of mass transfer coefficient. Since the concentration profile in the boundary layer is exponential in nature, a small error in the value of mass transfer coefficient may magnify error to a large extent. Hence, to develop a robust model for the FO process, there is crucial need to find an appropriate correlation of mass transfer coefficient for each specific membrane process with certain hydrodynamic properties of channel and membrane characteristics.

In this chapter an attempt has been made to provide (i) the theoretical background of internal and external concentration polarization phenomena, and (ii) different methods that can be used for the estimation of mass transfer coefficient in the FO process. Since the support layer of a thin film composite FO membrane is made from a porous material (e.g., polysulfone, PSf), having a similar structure and porosity as that of a UF membrane, the literature Sh number correlations might be valid on this side of the membrane. But for the selective layer of the membrane, which is smooth and non-porous, these relationships are not necessarily usable. Hence, more practical methods to get an estimate of the value of mass transfer coefficient on the active side of the membrane in an FO process by (i) RO and (ii) PRO experiments are proposed. These mass transfer coefficients can then be used in the theoretical model to predict the water flux with a change in the feed flow velocity.

2. Theory

2.1. Water flux in FO

Water flux in a pressure-driven membrane separation process is directly proportional to the applied pressure (Δp) and the osmotic pressure difference between the two solutions ($\Delta\pi$) [11].

$$J_w = A(\Delta p - \sigma\Delta\pi) \tag{1}$$

where A is the pure water permeability, and σ is the reflection coefficient which describes the fraction of the solutes reflected or rejected by the membrane. For ideal membranes with no solute transport, its value is unity. In an FO process, no pressure is applied ($\Delta p = 0$) and the

water flux through the membrane is just due to the difference in the osmotic pressures of the draw and feed solutions, given by:

$$J_w = A(\pi_{D,b} - \pi_{F,b}) \tag{2}$$

where $\pi_{D,b}$ and $\pi_{F,b}$ are the osmotic pressures of the draw and feed solutions, respectively.

2.2. Concentration polarization

In an FO operation, the actual flux is far less than the theoretical flux obtained from Eq. (2) which shows a decline in driving force. On the feed side, where the solvent permeates through the membrane, the solutes are retained by the membrane increasing their concentration on the membrane surface that is referred to as concentrative ECP. The permeate entering the draw side dilutes the draw solution at the membrane surface that is known as diluted ECP. **Figure 1(a)** and **(b)** depict concentrative and dilutive ECP, as well as ICP, occurring in FO and PRO processes. Both these phenomena contribute to a decrease in the net osmotic driving force across the membrane and hence lowering the flux.

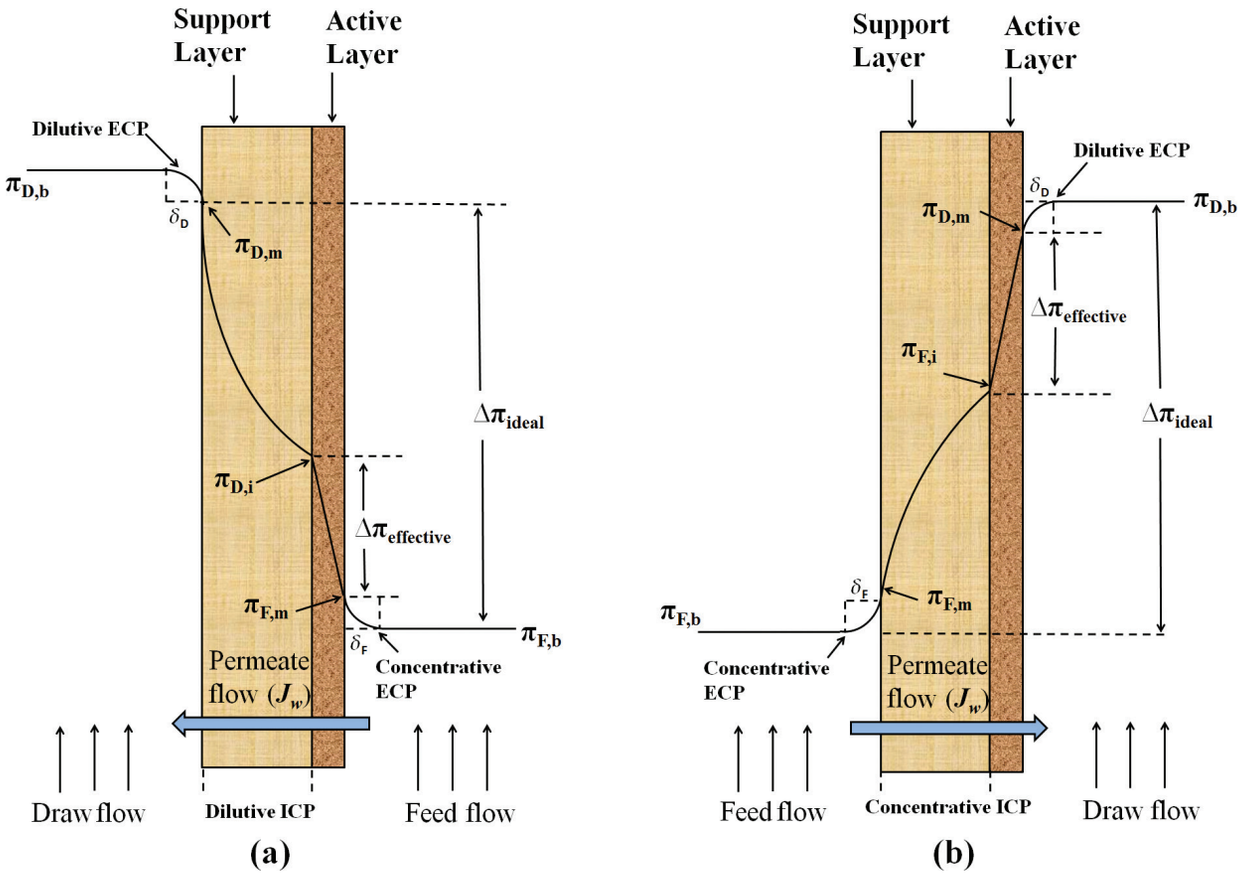

Figure 1. Direction of water flux and the concentration profile developed across the membrane in (a) FO mode and (b) PRO mode.

The ECP can be mitigated by inducing turbulence which enhances the mixing and consequently levels the concentration difference between the bulk and adjacent solution to the membrane surface. However, the concentration polarization in FO is not just limited to ECP. The structure of FO membranes is typically asymmetric, i.e. a thin active layer which governs the molecular transport rate is coated on a porous support that provides mechanical strength. In the FO mode (when active layer and support are facing the feed and draw solutions, respectively), a more severe concentration polarization takes places inside the porous support layer of the membrane, known as ICP. The enhanced dilution of the draw solution inside the porous support contributes to a massive decline in the osmotic pressure difference, thereby decreasing the flux more severely.

2.2.1. Internal concentration polarization

At steady state, the salt leakage (J_s) from the active layer (if the membrane is not perfect) originates from the convective flow of solute ($J_w c$) away from the active layer and diffusive flow of solute $D^{"}dc/dx$ toward the active layer due to concentration gradient inside the porous support [18]:

$$J_s = J_w c - D^{"} \frac{dc}{dx} \tag{3}$$

where c is the concentration of solute at any point inside support layer, $D^{"}$ is the salt diffusion coefficient in the porous support and is given by:

$$D^{"} = \frac{D\varepsilon}{\tau} \tag{4}$$

where D is the diffusivity of solute in water, and ε and τ are the porosity and tortuosity of the support, respectively. Appropriate boundary conditions (as shown in **Figure 2**) are represented as:

$$c = c_{D,i} \text{ at } x = 0$$

$$c = c_{D,m} \text{ at } x = t$$

Applying these boundary conditions a relation for the concentration of solution inside the porous support near the active layer ($c_{D,i}$) is derived as follows:

$$c_{D,i} = \frac{c_{D,m} + J_s/J_w}{\exp(J_w K)} - \frac{J_s}{J_w} \tag{5}$$

where $c_{D,m}$ is the concentration of solution on the support layer adjacent to the bulk solution. Here $K = \tau t/(D\varepsilon)$ is defined as the solute resistivity inside the porous support.

Considering a perfect membrane with 100% salt rejection, the value of J_s can be neglected, and Eq. (5) simplifies to:

$$c_{D,i} = \frac{c_{D,m}}{\exp(J_w K)} \tag{6}$$

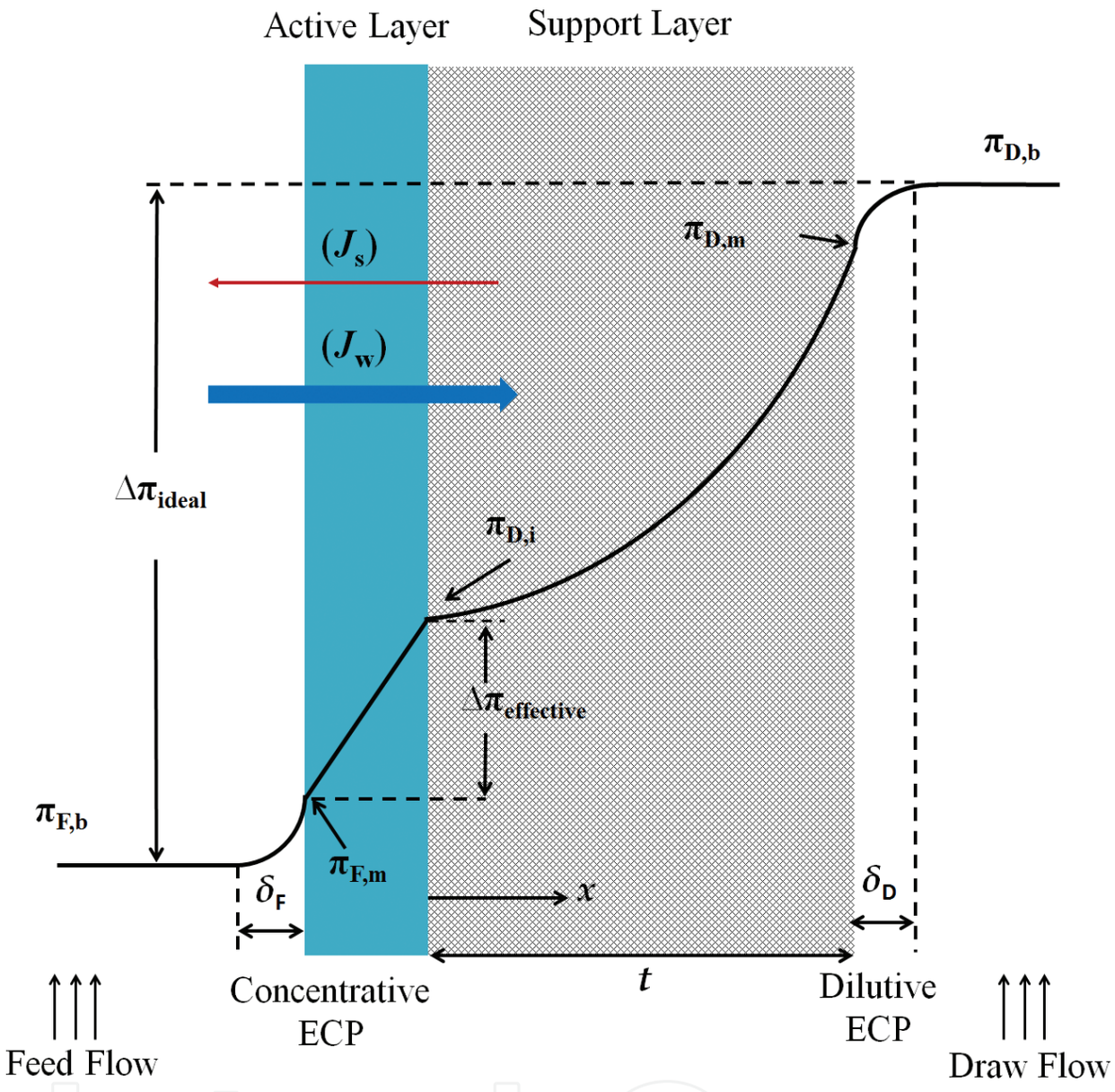

Figure 2. Concentration profiles (considering dilutive ECP) and the concentration boundary thickness developed on both sides of the membrane during an FO osmosis process.

The salt concentration ratio is approximately proportional to the osmotic pressure ratio of the solution, which gives:

$$\pi_{D,i} = \frac{\pi_{D,m}}{\exp(J_w K)} \tag{7}$$

The actual flux is generated by the concentration difference across the active layer of the membrane and is given by [1, 11]:

$$J_w = A(\pi_{D,i} - \pi_{F,m}) \tag{8}$$

Substituting Eq. (7) in Eq. (8), the following equation is obtained for the actual flux through the membrane:

$$J_w = A\left[\pi_{D,m}\exp(-J_w K) - \pi_{F,m}\right] \tag{9}$$

2.2.2. External concentration polarization

The concentrative ECP occurring on the feed side of the membrane can be captured by using the same differential equation and applying appropriate boundary conditions between the membrane surface and bulk solution on the feed side [1, 7]:

$$c = c_{F,b} \text{ at } x = 0$$

$$c = c_{F,m} \text{ at } x = \delta_F$$

where $c_{F,m}$ and $c_{F,b}$ are the concentrations of solute on the membrane surface and in the bulk feed solution, respectively. δ_F is the thickness of concentration boundary layer on the active layer of the membrane. Solving the differential equation and applying the above boundary conditions the following relation is derived for the electrolyte concentration on the membrane surface:

$$c_{F,m} = \left(c_{F,b} + \frac{J_s}{J_w}\right)\exp\left(\frac{J_w \delta_F}{D}\right) - \frac{J_s}{J_w} \tag{10}$$

Again for a high solute rejecting membrane $J_s \approx 0$, hence

$$c_{F,m} = c_{F,b}\exp\left(\frac{J_w \delta_F}{D}\right) \tag{11}$$

D/δ_F in this equation is mass transfer coefficient on the feed side of the membrane (k_F). By replacing the concentrations in Eq. (11) with the corresponding osmotic pressures and substituting this equation into Eq. (9), the following equation for flux is obtained:

$$J_w = A\left[\pi_{D,m}\exp(-J_w K) - \pi_{F,b}\exp\left(\frac{J_w}{k_F}\right)\right] \tag{12}$$

The effect of ICP in the support layer and ECP on the feed side are accounted in Eq. (12). By considering the effect of dilutive ECP on the draw side, a concentration boundary layer forms on the support layer of the membrane and $\pi_{D,m}$ will not be equal to $\pi_{D,b}$. Using appropriate boundary conditions:

$$c = c_{D,m} \text{ at } x = 0$$

$$c = c_{D,b} \text{ at } x = \delta_D$$

The following equation is derived for the concentration of solution on the support layer ($c_{D,m}$).

$$c_{D,m} = \left(c_{D,b} + \frac{J_s}{J_w}\right)\exp\left(-\frac{J_w \delta_D}{D}\right) - \frac{J_s}{J_w} \tag{13}$$

where $c_{D,b}$ is the bulk draw solution concentration and δ_D is the thickness of concentration boundary layer on the porous support. Applying similar assumption of $J_s \approx 0$ and inserting the mass transfer coefficient on the draw side of the membrane as $k_D = D/\delta_D$ we get:

$$c_{D,m} = c_{D,b} \exp\left(-\frac{J_w}{k_D}\right) \tag{14}$$

Finally, the modified flux equation by incorporating the ICP in the support layer and ECP on both sides of the membrane is acquired as follows:

$$J_w = A\left[\pi_{D,b} \exp(-J_w K) \exp\left(-\frac{J_w}{k_D}\right) - \pi_{F,b} \exp\left(\frac{J_w}{k_F}\right)\right] \tag{15}$$

A summary of the main mass transfer equations, boundary conditions, and concentration relations is presented in **Table 1**.

A similar analogy can be applied when the process is operated in the PRO mode. In this mode, the feed and draw solutions face the support and active layers, respectively. Hence, the ECP occurs on the draw side and is dilutive in nature, i.e. the draw solution becomes diluted near the membrane surface by the incoming permeate that leads to a decrease in osmotic driving force. The dilutive ECP phenomenon provides the following relation for the ratio of draw solution concentration on the membrane surface ($c_{D,m}$) and in the bulk solution ($c_{D,b}$) [7]:

$$\frac{c_{D,m}}{c_{D,b}} = \exp\left(-\frac{J_w}{k}\right) \tag{16}$$

where k is the mass transfer coefficient on the draw side of the membrane.

On the feed side of the membrane, the ICP occurs that increases the concentration of salt inside the porous support and makes it concentrative in nature, thus decreasing the driving force. The modulus for concentrative ICP is given by the following relation:

$$\frac{c_{F,i}}{c_{F,b}} = \exp(J_w K) \tag{17}$$

Assumption	Mass transfer equation	Boundary condition	Concentration relations
ICP in the support layer	$J_s = J_w c - D'' \frac{dc}{dx}$	$\begin{cases} x = t, & c = c_{D,m} \\ x = 0, & c = c_{D,i} \end{cases}$	$c_{D,i} = \frac{c_{D,m} + J_s/J_w}{\exp(J_w K)} - \frac{J_s}{J_w}$
ECP on the draw side	$J_s = J_w c - D'' \frac{dc}{dx}$	$\begin{cases} x = 0, & c = c_{D,m} \\ x = \delta_D, & c = c_{D,b} \end{cases}$	$c_{D,m} = \left(c_{D,b} + \frac{J_s}{J_w}\right) \exp\left(-\frac{J_w \delta_D}{D}\right) - \frac{J_s}{J_w}$
ECP on the feed side	$J_s = J_w c - D'' \frac{dc}{dx}$	$\begin{cases} x = 0, & c = c_{F,b} \\ x = \delta_F, & c = c_{F,m} \end{cases}$	$c_{F,m} = \left(c_{F,b} + \frac{J_s}{J_w}\right) \exp\left(\frac{J_w \delta_F}{D}\right) - \frac{J_s}{J_w}$

Table 1. A summary of governing equations and conditions considering both ECP and ICP [12].

where $c_{F,i}$ and $c_{F,b}$ are the concentrations of the feed solution inside the porous support close to the active layer and in the bulk solution, respectively. By incorporating the dilutive ECP and concentrative ICP phenomena in the PRO process, an analytical model, analogous to FO, is obtained as follows:

$$J_w = A\left[\pi_{D,b}\exp\left(-\frac{J_w}{k}\right) - \pi_{F,b}\exp\left(J_w K\right)\right] \tag{18}$$

3. Standard experiments to use the data analysis model

Draw solutions with various concentrations of a particular salt in deionized water are first prepared. Then, the properties of both feed and draw solutions like viscosity, density, diffusion coefficient, and osmotic pressure are measured or taken from literature [19]. The Osmotic pressure of unknown feed and draw solutions can be found experimentally by using automatic osmometers. This instrument estimates the osmotic pressure by measuring the depression in the freezing point of the solution. The osmotic pressure of at least three solutions is measured, and a linear relationship is obtained between the osmotic pressure and the concentration.

The FO experiments are conducted by a cross-flow filtration setup. The schematic diagram of a typical setup is shown in **Figure 3**. The membrane cell has channels on both sides of the membrane for the flow of feed and draw solutions. The length, width, and depth of the channels should be measured precisely for the calculation of mass transfer coefficient. The effective filtration area of the membrane is measured to calculate the water flux. Feed and permeate spacers are typically used on both draw and feed channels in the cell to provide mechanical

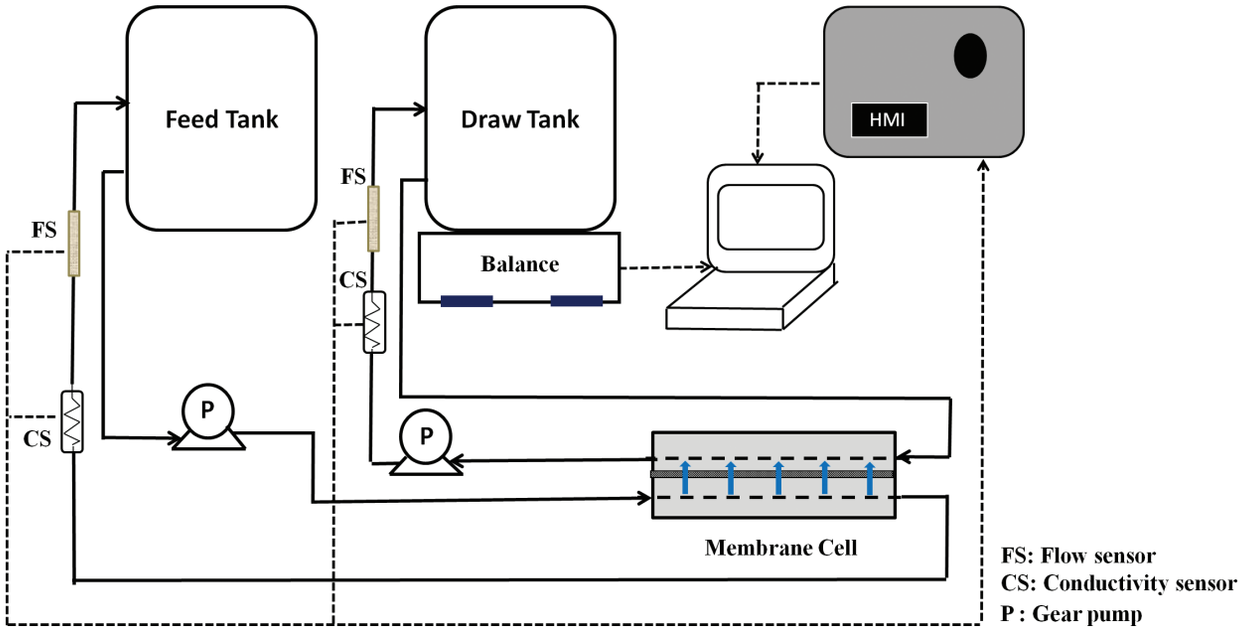

Figure 3. Schematic of a bench scale cross-flow FO setup.

support to the membrane. The feed and draw solution flow rates and the temperature of the experiment are maintained at certain values and are used for the calculation of mass transfer coefficients and osmotic pressure, respectively. The water flux through the membrane can be calculated by recording the change in the weight of the draw solution with time using a weighing scale. During the experiment, the conductivity and temperature of both feed and draw solutions must be monitored.

The same setup but opposite configuration is utilized for the PRO experiments. For both FO and PRO experiments, membranes are needed to be kept in the DI water for about 24 hours before experiments. After mounting the membranes in the module, the flow rates of the feed and the draw solutions are adjusted to desired values. The system is allowed to stabilize, and then the change in weight of the draw solution is recorded over time. Due to the change of draw solution concentration, a certain amount of concentrated draw solution needs to be gradually added to the solution. The conductivity of the draw solution is monitored online, and the addition of concentrated solution stopped when the conductivity of the draw solution reaches to the desired concentration of the solution. A similar procedure needs to be followed to increase the concentration the feed solution.

The pure water permeability of the membrane should be acquired using an RO setup with DI water as feed solution. The water flux is measured at different transmembrane pressures, and the slope is obtained as pure water permeability (A).

4. Estimation of mass transfer coefficient

The value of mass transfer coefficient depends on the hydrodynamics of the flow, applied driving force, water flux through the membrane, characteristics of the membrane (roughness and porosity) and the type of *solute* [14]. In this section, we provide three different methodologies to find the mass transfer coefficient: (i) empirical equations based on Sh number, (ii) pressure-driven method using RO, and (ii) osmotic pressure-driven method using PRO.

4.1. Empirical equations based on Sh number

Mass transfer coefficient is a parameter which describes the ratio between the actual mass (molar) flows of species into or out of a flowing fluid and the driving force that creates that flux. Mass transfer coefficient depends on module configuration, solute diffusion coefficient, viscosity, density, and velocity of feed solution [20]. It is related to the Sh number which shows the ratio of the convective mass transfer to diffusive rate and can be defined as follows [21]:

$$k = \frac{\mathrm{Sh} \cdot D}{d_h} = a\,\mathrm{Re}^b\,\mathrm{Sc}^c \left(\frac{d_h}{L}\right)^d \tag{19}$$

where a, b, c, and d are constants, D is the diffusion coefficient of solute in draw or feed solution, L is the length of the tube or channel, d_h is the hydraulic diameter of channel calculated

by ($2wh/(w + h)$) in which w and h are the width and the height of the channel. *Re* and *Sc* in Eq. (19) are Reynolds and Schmidt numbers, respectively.

$$\mathrm{Re} = \frac{\mathrm{d}_h \cdot v}{\nu} \tag{20}$$

$$\mathrm{Sc} = \frac{\nu}{D} = \frac{\mu}{\rho D} \tag{21}$$

In these equations, ν is the kinematic viscosity, μ is the dynamic viscosity, v is the flow velocity, and ρ is the flow density [20]. The mass transfer coefficient correlations are classified based on the channel flow geometry and various flow regimes in **Table 2**.

Eqs. (22)(a) and (b) are widely used to calculate the mass transfer coefficient in both feed and draw side of FO membrane. However, the implementation of these empirical equations in forward osmosis process has brought some controversial debates. These equations were derived based on ultrafiltration (UF) process which suffers more severely from concentration polarization phenomenon as compared to FO process. Hence, they are not necessarily valid for the evaluation of dilutive and concentrative ECP in FO [20]. Moreover, UF membranes differ from FO ones structurally as the former is porous while the latter is mainly dense composite membranes. Besides, the Sh number is correlated to the frictional factor which might be different for FO and UF processes [14, 19].

It is worth mentioning that Eq. (22)a is only valid where the length of the entry region is equal to $0.029 d_h Re$ while in most lab-scale FO cells the length of the channel is shorter than the entry

Flow geometry	Laminar regime (Re < 2000)-(a)	Turbulent regime (Re > 2000)-(b)	Equation
Rectangular channels w/o spacers	$Sh = 1.85\left(\mathrm{ReSc}\frac{d_h}{L}\right)^{0.33}$	$Sh = 0.04\mathrm{Re}^{0.75}\mathrm{Sc}^{0.33}$	(22)
Rectangular channels w/ spacers	$Sh = 0.46(\mathrm{ReSc})^{0.36}$	$Sh = 0.0096\mathrm{Re}^{0.5}\mathrm{Sc}^{0.6}$	(23)
Tube	$Sh = 1.62\left(\mathrm{ReSc}\frac{d_h}{L}\right)^{0.33}$	$Sh = 0.023\mathrm{Re}^{0.83}\mathrm{Sc}^{0.33}$	(24)
Radial cross flow system	$Sh = 1.05\left(\mathrm{ReSc}\frac{h}{R_c}\right)^{0.38}$	$Sh = 0.275\left(\mathrm{Re}^{1.75}\,\mathrm{Sc}\frac{2h}{L}\right)^{0.33}$	(25)*
Stirred cell	$Sh = 0.23\mathrm{Re}^{0.567}\mathrm{Sc}^{0.33}$	$Sh = 0.03\,\mathrm{Re}^{0.66}\,\mathrm{Sc}^{0.33}\,\mathrm{Pe}_{\mathrm{test}}^{0.16}$	(26)**

*R_c is the radius of the flow channel and h is the half channel height.
**$\mathrm{Pe}_{\mathrm{test}}$ is the test Peclet number which is equal to ($J_w h/D$).

Table 2. Mass transfer coefficient for different flow regimes and geometry [22].

length. Therefore, this equation does not seem to be suitable for investigating the transport phenomena in the lab-scale. Regarding Eq. (22)b, it was derived based on the pressure drop during turbulent flow in RO and UF experiments, whereas in FO process, the pressure drop is insignificant due to the absence of hydraulic pressure [13, 19]. Hence, a significant amount of research is underway to modify the common Sh number equations in the literature. For example, Tan and Ng [19] proposed an exact solution to evaluate the local mass transfer coefficient for the hydrodynamic boundary layer in FO process. The local Sh number was derived from the Navier-Stokes equations for the fluid flow parallel to a flat and non-porous surface as follows:

Laminar boundary layer

$$Sh = 0.332\,\mathrm{Re}_y^{1/2}\,\mathrm{Sc}^{1/3} \quad \mathrm{Re} \le 2\times10^5 \tag{27}$$

Turbulent boundary layer

$$Sh = 0.0292\,\mathrm{Re}_y^{0.8}\,\mathrm{Sc}^{0.33} \quad \mathrm{Re} > 2\times10^5 \tag{28}$$

Hence, mean mass transfer coefficient, k_c, can be obtained as follows:

$$k_c = \frac{\int_0^L k\,\mathrm{d}y}{\int_0^L \mathrm{d}y} = \frac{0.664D\,\mathrm{Re}_t^{1/2}\,\mathrm{Sc}^{1/3} + 0.0365D\,\mathrm{Sc}^{1/3}\left[\mathrm{Re}_L^{4/5} - \mathrm{Re}_t^{4/5}\right]}{L} \tag{29}$$

where, Re_t and Re_L are the transition Reynolds number and Reynolds number at L, respectively, and L is the length of the channel. Experimental investigation showed that the mass transfer coefficient developed from boundary layer concept (k_c) provided more accurate results as compared to that obtained from UF experiments in Eq. (22).

4.2. Evaluating mass transfer coefficient by RO experiment

The film theory is generally applied to capture the effect of the ECP on a membrane surface. Using this theory, the concentration profile near the membrane surface is obtained as a function of permeation flux and mass transfer coefficient:

$$J_w = k\ln\left(\frac{c_m}{c_b}\right) \tag{30}$$

where c_m and c_b are the concentration at the membrane surface and in bulk, respectively. By estimating the concentration at the membrane surface the value of mass transfer coefficient is calculated using Eq. (30). The concentration at the membrane surface can be calculated from the osmotic pressure difference across the membrane. By measuring the water flux and salt rejection in an RO experiment and coupling these with the pure water flux, an estimate of the osmotic pressure difference across the membrane can be made, and consequently, the mass transfer coefficient is calculated by the following equation:

$$k = \frac{1}{J_w}\ln\left(\frac{\Delta\pi}{2R_g T c_b R_j}\right) \tag{31}$$

where R_j is the salt rejection by the membrane, R_g is the universal gas constant, and T is absolute temperature. The detailed procedure to derive Eq. (31) is described elsewhere [23].

4.3. Evaluating mass transfer coefficient in the PRO mode

Using DI water as the feed solution in the PRO mode, the water flux through the membrane can be calculated by a reduced form of Eq. (18) as follows:

$$J_w = A\left[\pi_{D,b}\exp\left(-\frac{J_w}{k}\right)\right] \tag{32}$$

The mass transfer coefficient can be calculated by rearranging this equation.

5. Flux prediction

The current models developed are mainly focused on finding an accurate value of solute resistivity (K), and very less attention has been paid to find a proper value of mass transfer coefficient for FO [7, 11, 12]. There are no direct techniques to determine the value of the structural parameters of a membrane, primarily porosity and tortuosity, so its value is typically evaluated by fitting the experimental data to the transport model [24]. In this technique, the value of K directly depends upon the mass transfer coefficient. Hence, there is a crucial need for finding an accurate value of mass transfer coefficient.

Investigating the current models developed for FO, it was also observed that they are insensitive to a change in the feed flow rate, while our earlier investigations demonstrated that the flux changes moderately with the flow rate [25]. In the previous sections, it was shown that the mass transfer coefficients could be obtained by three methods. Hence, it is suggested that the researchers critically compare the results obtained from the three sets of mass transfer coefficient and utilize the one that increases the sensitivity of the flux results to the feed flow rate.

To start with the modeling of the FO, the hydraulic permeability (A) and salt resistivity of the support layer (K) needs to be determined. The hydraulic permeability of the membrane is determined by the RO setup as discussed earlier. Salt resistivity coefficient depends upon the structural parameters of the membrane, such as porosity, tortuosity, and thickness and on the diffusion coefficient of salt (D). Since the structural parameter is an intrinsic property of the membrane, it is assumed to be constant for a particular membrane [7, 11]. The salt diffusion coefficient is also constant at a specific temperature and is not changing significantly in a narrow range of molarities [26, 27]. Hence, the value of K at a particular temperature is constant and can be evaluated by rearranging Eq. (15). As an example, **Table 3** presents the experimental FO data that is used to determine the value of K for a thin film composite FO membrane. In this experimental research, DI water and NaCl are used as feed and draw solutions, respectively. The detailed properties of the membrane are presented elsewhere [28]. All experiments were conducted at 23°C and the values of mass transfer coefficients obtained

Draw concentration (M)	Osmotic pressure (draw side) (bar)	Feed concentration (M)	Osmotic pressure (feed side) (bar)	Flux (LMH)	K (s/m) × 10^5
1.5	75.4	0.05	2.05	10.2	6.99
1.5	75.4	0.1	4.13	9.0	6.70
1.5	75.4	0.25	10.57	6.4	6.8
1.5	75.4	0.5	21.7	4.2	6.73
1.5	75.4	1.0	47.9	1.5	7.14
Average	—	—	—	—	6.9

Table 3. FO experiments for calculation of K. Tests were conducted at 23°C.

from RO test were used for the calculation of K. As expected, the K values were almost constant for different feed concentrations. Hence, the average K value of 6.9 can be reasonably used for prediction of water flux.

Obtaining hydraulic permeability (A), salt resistivity of the support layer (K), and mass transfer coefficients of both feed and permeate side (k_D and k_F) the model water flux is calculated by Eq. (15). A typical representation of matching between theoretical and experimental results is to plot the model predicted values of water flux along with the experimental values as a function of the driving force (osmotic pressure of the draw solution), as shown in **Figure 4**.

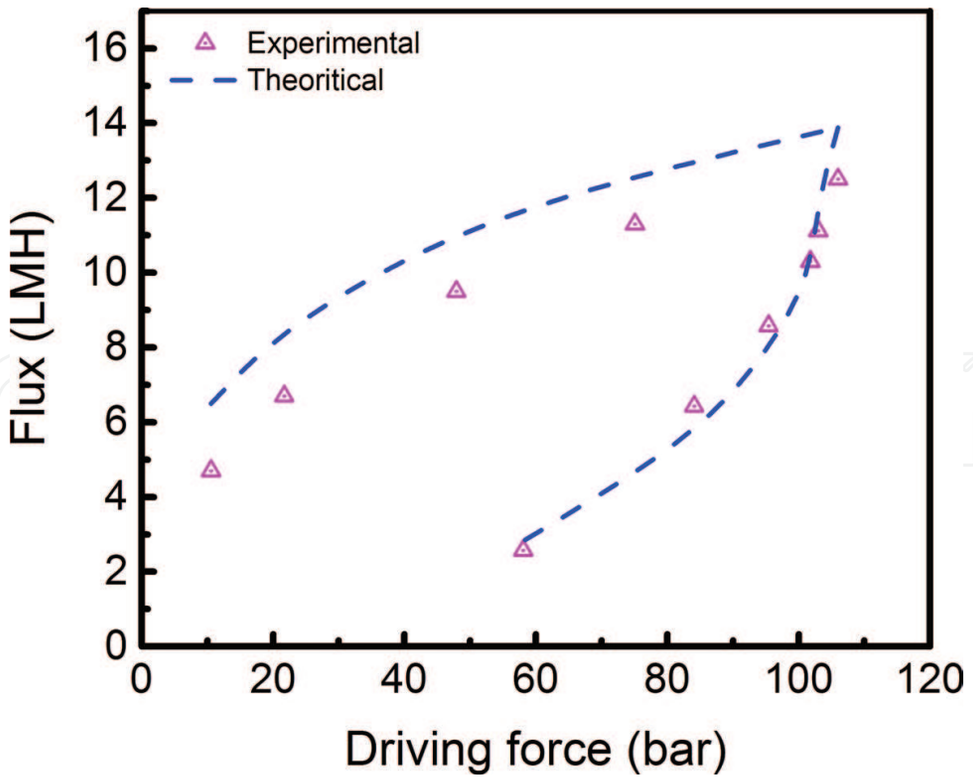

Figure 4. Typical comparison of experimental FO data and predicted fluxes by the model as a function of osmotic driving forces.

Draw concentration	Feed concentration	Experimental flux (LMH)		Theoretical flux (LMH) (*k* from RO experiment)		Theoretical flux (LMH)* (*k* from Sh number in Eq. (22))	
		Feed flow 1 LPM	Feed Flow 3 LPM	Feed flow 1 LPM	Feed flow 3 LPM	Feed flow 1 LPM	Feed flow 3 LPM
0.25 M	0.05 M	3.9	4.5	3.8	4.2	4.1	4.1
0.5 M	0.05 M	5.6	7.7	5.8	6.4	6.1	6.1
1 M	0.05 M	8.7	10.1	8.2	9.0	8.5	8.5
1.5 M	0.05 M	9.9	11.6	9.6	10.6	9.9	9.9

*The value of *K* for this case was found using Eq. (15).

Table 4. The sensitivity of the model to predict change in flux with the change in the values of ***k*** with the experimental results.

It is well known that increasing the feed flow rate increases the water flux through the membrane by enhancing the mixing near the membrane surface, thereby reducing the effect of ECP (concentrative ECP in the case of FO). The change in the flow rate is reflected through the change in the mass transfer coefficient. Hence it is recommended to test the sensitivity of the FO developed model to the variation of feed flow rate. As a case study, the experimental results and the model predictions obtained using two mass transfer coefficients, one from Eq. (22) and the other one from RO tests, are presented in **Table 4**. As can be observed, mass transfer coefficients yield results that match well with experimental data. However, using the values of *k* obtained from Eq. (22), the fluxes were found to be insensitive to flow rates, whereas *k* values evaluated by RO experiment resulted in more reasonable predictions at higher feed flow rate as well.

6. Conclusion

In this chapter, the governing equations of transport through an FO membrane were presented based on the mass balance in the concentration boundary layers on both sides of the membrane (ECP) and inside the support layer (ICP). Although ICP is reported in the literature to play a significant role in the reduction of the effective osmotic driving force, the impact of ECP is usually underestimated. The ECP primarily depends upon the value of mass transfer coefficient (*k*), and the exponential nature of concentration profile in the boundary layer makes ECP very sensitive to the value of *k*. Hence, another theme of this chapter was to provide appropriate methods for the estimation of mass transfer coefficient. Previous studies were all based on using the Sh number correlation developed from the UF experiments to predict the flux in the FO process. The main shortcoming of these studies was the insensitivity of the model predictions to a change in the feed flow rate. Hence other experimental methods based on RO and PRO were proposed to provide a better estimation of mass transfer coefficient. In summary, the results obtained in this study suggest that both

ECP and ICP play a key role in the performance of FO membrane and thus the mass transfer coefficient (*k*) which mainly affects the ECP is as important as solute resistivity (*K)* which is reflected in the ICP effect.

Acknowledgements

The authors gratefully acknowledge the financial support provided by the Natural Sciences and Engineering Research Council of Canada (NSERC) and Canada's Oil Sands Innovation Alliance (COSIA).

Nomenclature

A	pure water permeability ($Lm^{-2}\ h^{-1}\ bar^{-1}$)
B	solute permeability ($Lm^{-2}\ h^{-1}$)
c	concentration of solute ($mol\ L^{-1}$)
d_h	hydraulic diameter (m)
D	diffusion coefficient ($m^2\ s^{-1}$)
n	van't Hoff factor
J	flux ($Lm^{-2}\ h^{-1}$)
k	mass transfer coefficient (ms^{-1})
K	solute resistivity (m)
L	length of channel (m)
p	hydraulic pressure (bar)
R_g	universal gas constant ($Jmol^{-1}\ K^{-1}$)
R_j	salt rejection
Re	Reynolds number
Re_L	Reynolds number at the end of membrane channel
Re_t	transition Reynolds number
Sc	Schmidt number
Sh	Sherwood number
T	absolute temperature (K)

Greek symbols

δ	thickness of ECP boundary layer (m)
ε	porosity of membrane support
μ	dynamic viscosity (Pa.s)
ν	kinematic viscosity ($m^2\ s^{-1}$)
ρ	density of water ($kg\ m^{-3}$)
τ	tortuosity of membrane support
π	osmotic pressure (bar)
σ	reflection coefficient
v	velocity (ms^{-1})

Subscripts

b	bulk solution
D	draw solution
F	feed solution
i	interface between support layer and active layer of membrane
m	membrane surface
s	solute
v	pure water
w	water

Author details

Amrit Bhinder, Simin Shabani and Mohtada Sadrzadeh*

*Address all correspondence to: sadrzade@ualberta.ca

Department of Mechanical Engineering, Donadeo Innovation Center for Engineering, Advanced Water Research Lab (AWRL), University of Alberta, Edmonton, AB, Canada

References

[1] Klaysom C, Cath TY, Depuydt T, Vankelecom IFJ. Forward and pressure retarded osmosis: Potential solutions for global challenges in energy and water supply. Chemical Society Reviews. 2013;**42**:6959-6989. DOI: 10.1039/c3cs60051c

[2] Chung T-S, Li X, Ong RC, Ge Q, Wang H, Han G. Emerging forward osmosis (FO) technologies and challenges ahead for clean water and clean energy applications. Current Opinion in Chemical Engineering. 2012;**1**:246-257. DOI: 10.1016/j.coche.2012.07.004

[3] Cath T, Childress A, Elimelech M. Forward osmosis: Principles, applications, and recent developments. Journal of Membrane Science. 2006;**281**:70-87. DOI: 10.1016/j.memsci.2006.05.048

[4] Hickenbottom KL, Hancock NT, Hutchings NR, Appleton EW, Beaudry EG, Xu P, et al. Forward osmosis treatment of drilling mud and fracturing wastewater from oil and gas operations. Desalination. 2013;**312**:60-66. DOI: 10.1016/j.desal.2012.05.037

[5] Lutchmiah K, Verliefde a RD, Roest K, Rietveld LC, Cornelissen ER. Forward osmosis for application in wastewater treatment: A review. Water Research. 2014;**58**:179-197. DOI: 10.1016/j.watres.2014.03.045

[6] McCutcheon JR, McGinnis RL, Elimelech M. A novel ammonia—Carbon dioxide forward (direct) osmosis desalination process. Desalination. 2005;**174**:1-11. DOI: 10.1016/j.desal.2004.11.002

[7] Mccutcheon JR, Elimelech M. Modeling water flux in forward osmosis: Implications for improved membrane design. AICHE Journal. 2007;**53**:1736-1744. DOI: 10.1002/aic

[8] Mehta GD, Loeb S. Internal polarization in the porous substructure of a semipermeable membrane under pressure retarded osmosis. Journal of Membrane Science. 1978;**4**:261-265. DOI: 10.1016/S0376-7388(00)83301-3

[9] Lee KL, Baker RW, Lonsdale HK. Membranes for power generation by pressure-retarded osmosis. Journal of Membrane Science. 1981;**8**:141-171. DOI: 10.1016/S0376-7388(00)82088-8

[10] Loeb S, Titelman L, Korngold E, Freiman J. Effect of porous support fabric on osmosis through a Loeb-Sourirajan type asymmetric membrane. Journal of Membrane Science. 1997;**129**:243-249. DOI: 10.1016/S0376-7388(96)00354-7

[11] McCutcheon JR, Elimelech M. Influence of concentrative and dilutive internal concentration polarization on flux behavior in forward osmosis. Journal of Membrane Science. 2006;**284**:237-247. DOI: 10.1016/j.memsci.2006.07.049

[12] Suh C, Lee S. Modeling reverse draw solute flux in forward osmosis with external concentration polarization in both sides of the draw and feed solution. Journal of Membrane Science. 2013;**427**:365-374. DOI: 10.1016/j.memsci.2012.08.033

[13] van den Berg GB, Racz IG, Smolders CA. Mass transfer coefficients in cross-flow ultrafiltration. Journal of Membrane Science 1989;**47**:25-51. doi:10.1016/S0376-7388(00)80858-3

[14] Gekas V, Hallstrom B. Mass transfer in the membrane concentration polarization layer under turbulent cross flow. Journal of Membrane Science. 1987;**30**:153-170. DOI: 10.1016/S0376-7388(00)81349-6

[15] Belfort G, Nagata N. Fluid mechanics and cross-flow filtration: Some thoughts. Desalination. 1985;**53**:57-79. DOI: 10.1016/0011-9164(85)85052-9

[16] Koutsou CP, Yiantsios SG, Karabelas AJ. A numerical and experimental study of mass transfer in spacer-filled channels: Effects of spacer geometrical characteristics and Schmidt number. Journal of Membrane Science. 2009;**326**:234-251. DOI: 10.1016/j.memsci.2008.10.007

[17] Rodrigues C, Rodrigues M, Semiao V, Geraldes V. Enhancement of mass transfer in spacer-filled channels under laminar regime by pulsatile flow. Chemical Engineering Science. 2015;**123**:536-541. DOI: 10.1016/j.ces.2014.11.047

[18] Phillip WA, Yong JS, Elimelech M. Reverse draw solute permeation in forward osmosis: Modeling and experiments. Environmental Science and Technology. 2010;**44**:5170-5176. DOI: 10.1021/es100901n

[19] Tan CH, Ng HY. Modified models to predict flux behavior in forward osmosis in consideration of external and internal concentration polarizations. Journal of Membrane Science. 2008;**324**:209-219. DOI: 10.1016/j.memsci.2008.07.020

[20] Mulder M. Basic Principles of Membrane Technology. 2nd ed. Dordrecht: Kluwer Academic; 1996. DOI: 10.1007/978-94-009-1766-8

[21] Heldman DR, Moraru CI. Encyclopedia of Agricultural, Food, and Biological Engineering. 2nd ed. New York: Taylor & Francis; 2010. DOI: 10.1081/E-EAFE2

[22] Wang J, Dlamini DS, Mishra AK, Pendergast MTM, Wong MCY, Mamba BB, et al. A critical review of transport through osmotic membranes. Journal of Membrane Science. 2014;**454**:516-537. DOI: 10.1016/j.memsci.2013.12.034

[23] Al Mamun MA, Sadrzadeh M, Chatterjee R, Bhattacharjee S, De S. Colloidal fouling of nanofiltration membranes: A novel transient electrokinetic model and experimental study. Chemical Engineering Science. 2015;**138**:153-163. DOI: 10.1016/j.ces.2015.08.022

[24] Manickam SS, Mccutcheon JR. Model thin film composite membranes for forward osmosis: Demonstrating the inaccuracy of existing structural parameter models. Journal of Membrane Science. 2015;**483**:70-74. DOI: 10.1016/j.memsci.2015.01.017

[25] Bhinder A, Fleck BA, Pernitsky D, Sadrzadeh M. Forward osmosis for treatment of oil sands produced water: Systematic study of influential parameters. Desalination and Water Treatment. 2016;**57**:22980-22993. DOI: 10.1080/19443994.2015.1108427

[26] Lobo V. Mutual diffusion coefficients in aqueous electrolyte solutions. Pure and Applied Chemistry. 1993;**65**:2613-2640. DOI: 10.1351/pac199365122613

[27] Vitagliano V, Lyons PA. Diffusion coefficients for aqueous solutions of sodium chloride and barium chloride. Journal of the American Chemical Society. 1956;**76**:1549-1552. DOI: 10.1021/ja01589a011

[28] Khorshidi B, Bhinder A, Thundat T, Pernitsky DJ, Sadrzadeh M. Developing high throughput thin film composite polyamide membranes for forward osmosis treatment of SAGD produced water. Journal of the American Chemical Society. 2016;**511**:29-39. DOI: 10.1016/j.memsci.2016.03.052

IntechOpen